Journal of Inorganic Biochemistry 133 (2014) 40–49

Contents lists available at ScienceDirect

Journal of Inorganic Biochemistry

journal homepage: www.elsevier.com/locate/jinorgbio

Multiple spectroscopic and magnetic techniques show that chloroquine induces formation of the μ-oxo dimer of ferriprotoporphyrin IX

David Kuter, Stefan J. Benjamin, Timothy J. Egan *

Department of Chemistry, University of Cape Town, Private Bag, Rondebosch 7701, South Africa

ARTICLE INFO

Article history:
Received 9 September 2013
Received in revised form 3 January 2014
Accepted 7 January 2014
Available online 16 January 2014

Keywords:
Chloroquine
Ferriprotoporphyrin IX
Heme
Magnetic circular dichroism
MCD

ABSTRACT

Interaction of the antimalarial chloroquine (CQ) with ferriprotoporphyrin IX, Fe(III)PPIX, was investigated in aqueous solution (pH 7.4) and as a precipitate from aqueous medium at pH 5.0. In solution, spectrophotometric titrations indicated strong association ($\log K_{obs}$ 13.3 ± 0.2) and a Job plot gave a stoichiometry of 1:2 CQ:Fe(III)PPIX. UV–visible absorbance and magnetic circular dichroism spectra of the complex were compared to various Fe(III)PPIX species. Close similarity to the spectra of the μ-oxo dimer, μ-[Fe(III)PPIX]$_2$O, was revealed. The induction of this species by CQ was confirmed by magnetic susceptibility measurements using the Evans NMR method. The observed low-magnetic moment (2.25 ± 0.02 μ_B) could only be attributed to antiferromagnetically coupled Fe(III) centers. The value was comparable to that of μ-[Fe(III)PPIX]$_2$O (2.0 ± 0.1 μ_B). In the solid-state, mass spectrometry confirmed the presence of CQ in the complex. Dissolution of this solid in aqueous solution (pH 7.4) resulted in a solution with a UV–visible spectrum consistent with the same 1:2 stoichiometry observed in the Job plot. Magnetic susceptibility measurements made on the solid using an Evans balance produced a magnetic moment (2.3 ± 0.1 μ_B) consistent with that in solution. Diffusion coefficients of CQ and its complex with Fe(III)PPIX were measured in aqueous solution (3.3 ± 0.3 and 0.6 ± 0.2 × 10^{-10} $m^2 \cdot s^{-1}$, respectively). The latter was used in conjunction with an empirical relationship between diffusion coefficient and molar volume to estimate the degree of aggregation. The findings suggest the formation of a 2:4 CQ:Fe(III)PPIX complex in aqueous solution at pH 7.4.

1. Introduction

Chloroquine (CQ) is the archetypal hemozoin-inhibiting antimalarial and is still the focus of much research despite widespread resistance to this drug. This is because there is no evidence of a change in the drug target. Rather, a large body of evidence has shown that parasite resistance arises from transport of CQ away from the acidic digestive vacuole (DV), its site of action, by the *Plasmodium falciparum* chloroquine resistance transporter (PfCRT) [1,2]. Indeed, incubating CQ-resistant parasites with verapamil, an inhibitor of CQ transport by PfCRT [3], restores CQ-sensitivity [4]. Furthermore, a number of other clinical antimalarials including some recently introduced or under development such as piperaquine and ferroquine likely act, at least in part against the same target and do not exhibit cross-resistance with CQ [5,6].

CQ inhibits detoxification of ferriheme (Fe(III)PPIX) produced as a by-product of host hemoglobin degradation by the malaria parasite in the DV [7], reported to have a pH in the range 4.8–5.2 [8]. This detoxification process involves the conversion of Fe(III)PPIX to hemozoin, an insoluble crystalline solid [9]. The mechanism by which CQ inhibits hemozoin formation is still not completely understood. There are two prominent views, namely inhibition of the fastest growing face of the hemozoin crystal as a result of adsorption onto the surface [10], or by formation of a CQ–Fe(III)PPIX complex in solution. Regardless of the mechanism of inhibition, the resulting free Fe(III)PPIX likely exists as a CQ–Fe(III)PPIX complex in solution, at least within the DV where concentrations of CQ are expected to be high as a result of pH trapping [11,12]. For this reason, the molecular details of the complex remain of great interest.

The interaction of CQ and Fe(III)PPIX has been previously investigated using a broad range of experimental techniques such as UV–visible [13,14], infrared (IR) [15], Raman [16,17], EXAFS (extended X-ray absorption fine structure) [18], NMR [19–21] and Mössbauer [22] spectroscopies as well as mass spectrometry [23] and isothermal titration calorimetry (ITC) [24,25]. These investigations have been conducted in both the solid- and solution-state, often spanning wide pH ranges and incorporating various solvents such as methanol and DMSO or detergents. The combination of varying experimental conditions between studies as well as reliance in some investigations on only a single experimental technique, has led to conflicting conclusions. For instance, reported binding stoichiometries of the CQ–Fe(III)PPIX complex in solution have ranged from 1:1 to 1:8 [13,19,24,26]. Further controversy has revolved around the identity of the Fe(III)PPIX species in the CQ–Fe(III)PPIX complex. Some studies have concluded that Fe(III)PPIX is a monomer while others have suggested that it is a μ-oxo dimer, μ-[Fe(III)PPIX]$_2$O [27]. These investigations, however, have been complicated

* Corresponding author. Tel.: +27 21 650 2528; fax: +27 21 650 5195.
E-mail address: timothy.egan@uct.ac.za (T.J. Egan).

0162-0134/$ – see front matter © 2014 Elsevier Inc. All rights reserved.
http://dx.doi.org/10.1016/j.jinorgbio.2014.01.002

by the fact that speciation of Fe(III)PPIX in solution is greatly influenced by the solvent and pH [28,29]. Additional complication has arisen from reports that the Fe(III)PPIX species is not in the μ-[Fe(III)PPIX]$_2$O form when the CQ–Fe(III)PPIX complex is precipitated at more biologically relevant pH (~5) [15]. These authors have suggested that changes to Fe(III)PPIX speciation in the solid-state could occur during the drying process. Thus there is much confusion regarding the interaction of CQ with Fe(III)PPIX in both solution and solid-state.

The present study comprehensively investigates the nature of the CQ–Fe(III)PPIX complex. This has been approached using multiple experimental techniques in purely aqueous solution in order to avoid solvent-induced changes to Fe(III)PPIX speciation and to better mimic biological conditions. Interaction of CQ with Fe(III)PPIX was investigated in solution at pH 7.4 and in the solid-state as a precipitate obtained at pH 5.0. The species of Fe(III)PPIX and the CQ:Fe(III)PPIX stoichiometry of the complex in both solution and solid-state have been identified using UV–visible and magnetic circular dichroism (MCD) spectroscopy, as well as by magnetic susceptibility measurements using the Evans NMR method and an Evans balance. We further report the association constant and diffusion coefficient for the complex in aqueous solution. The latter was used to estimate the extent of aggregation of the complex. We conclude that the complex formed in aqueous solution at pH 7.4 is identical to the precipitate obtained from aqueous solution at pH 5.0 and that Fe(III)PPIX exists as μ-[Fe(III)PPIX]$_2$O in both, with a stoichiometry of 1:2 CQ:Fe(III)PPIX.

2. Materials and methods

2.1. Materials and instrumentation

All materials were purchased from Sigma-Aldrich, with the exception of hemin (Cl-Fe(III)PPIX, Fluka) and D_2O (Merck). Reagents were of analytical grade and were used without further purification. Unless otherwise stated, the CQ used was the diphosphate salt. The free base form of CQ was prepared from the diphosphate salt by adding 2 M NaOH to an aqueous CQ solution (0.2 M) and extracting the resultant free base into dichloromethane. The organic layer was separated, dried over $MgSO_4$ and removed under vacuum. The resulting oil was dried over phosphorous pentoxide, washed with a small quantity of diethyl ether and dried once more under vacuum. This afforded CQ free base as a white solid. All Fe(III)PPIX solutions were freshly prepared and stored in the dark until use. To avoid buildup of adsorbed Fe(III)PPIX, all apparatus that came into contact with Fe(III)PPIX were scrupulously washed as previously described [28].

UV–visible spectra were recorded on a Varian Cary 100 or Shimadzu UV1800 UV–visible spectrophotometer. Spectrophotometric titrations and Job plots were performed in quartz cuvettes with 1 cm and 0.1 cm pathlengths, respectively. These were conducted at temperatures of 25.0 or 30.0 ± 0.2 °C maintained with a thermostated water bath. MCD spectra were recorded at room temperature on a Chirascan-Plus CD spectrophotometer (operating wavelength range 165–1100 nm) using a MCD accessory calibrated at 0.977 T. IR spectra were recorded on a Perkin Elmer Spectrum 100 FT-IR spectrophotometer using an ATR attachment. NMR measurements were performed on a Bruker Ultrashield 400 Plus NMR spectrometer at 30 °C. Mass spectrometry was performed on an Agilent 6530 QTOF LCMS system coupled with an Agilent 290 Infinity UHPLC equipped with an Eclipse Plus C18 column (50 × 2.1 mm, 1.8 μm). The pH of solutions was measured using a Crison MicropH 2000 or Jenway 3510 pH meter.

2.2. Preparation of Fe(III)PPIX and CQ–Fe(III)PPIX species

The solid precipitate of Fe(III)PPIX was obtained by slowly adding 50 μL aliquots of acetic acid (1.75 M) to a hematin solution (11.5 mM prepared in 0.1 M NaOH) until a measured pH of 5.0 was obtained. The precipitate was centrifuged at 4000 rpm for 20 min, the supernatant discarded and the precipitate washed by resuspension in water. This suspension was centrifuged, the supernatant discarded and washing repeated once more. After the final washing, the precipitate was left to dry in a desiccator over phosphorous pentoxide. The solid precipitate in the presence of CQ was obtained following the same procedure except solid CQ (free base) was added to the initial hematin solution to give a concentration of 58.5 mM. CQ was used in its free base form in order to eliminate the possible presence of phosphate in the solid which can obscure peaks in the IR spectrum of the CQ–Fe(III)PPIX complex. To obtain a solid sample of μ-[Fe(III)PPIX]$_2$O a tetrasodium salt was prepared according to a procedure modified from Brown et al. [30]. Briefly, this involved dissolving hematin (100 mg) in DMSO (2 mL) and adding 5 M NaOH (0.5 mL) with warming. The solution was then cooled and a large excess of acetone added to produce a precipitate. This was filtered, washed with acetone, and air dried and finally traces of moisture were removed at 100 °C. The high pH form of HO-Fe(III)PPIX was obtained by lyophilization of an aqueous solution containing hemin (23 mM) and NaOH (0.07 M). This produces Na_2[HO-Fe(III)PPIX] and NaCl.

2.3. Spectrophotometric titrations

Titrations were conducted in aqueous solution buffered to pH 7.4 using 4-(2-hydroxyethyl)-1-piperazineethanesulfonic acid (HEPES, 0.02 M). A 50 μL Hamilton syringe was used to make additions to the working solution. Titrations were performed by adding aliquots of an aqueous Fe(III)PPIX solution (1 mM in 0.02 M HEPES) to an aqueous CQ working solution (0.02 mM in 0.02 M HEPES). The Fe(III)PPIX solution was made by diluting a hemin stock solution (20 mM in 0.1 M NaOH) with 0.02 M aq. HEPES. The CQ working solution was made by diluting a CQ stock solution (0.08 mM in 0.02 M HEPES) in 0.02 M aq. HEPES. Spectrophotometric titration data were analyzed using the HypSpec software package (Hyperquad) [31] according to a 1:2 CQ:Fe(III)PPIX model as determined from Job plot experiments (see Results).

2.4. CQ–Fe(III)PPIX binding stoichiometry

Job plots were conducted in triplicate by varying the mole fraction of Fe(III)PPIX and CQ in the same aqueous solvent system used for spectrophotometric titrations, subject to the constraint that the total additive concentration of Fe(III)PPIX and CQ remained 0.2 mM. The stock Fe(III)PPIX solution (2 mM in 0.015 M NaOH) and CQ solution (2 mM in 0.2 M HEPES) were used to make fifteen working solutions with Fe(III)PPIX mole fractions of 1.00, 0.95, 0.90, 0.85, 0.80, 0.75, 0.70, 0.65, 0.60, 0.50, 0.40, 0.30, 0.20, 0.10 and 0.00. The working solutions consisted of (i) a combined volume of CQ and Fe(III)PPIX solutions of 0.1 mL (individual volumes based on the mole fraction required); (ii) an aliquot of HEPES buffer (0.2 M, pH 7.4) equal to the difference in volume between 0.1 mL and the volume of CQ solution added; (iii) an aliquot of NaOH (0.015 M) equal to the difference in volume between 0.1 mL and the volume of Fe(III)PPIX solution added; and (iv) 0.8 mL water. Solutions gave a measured pH in the range 7.5–7.6. The UV–visible spectrum of each solution was recorded in a 0.1 cm pathlength quartz cuvette at 25.0 or 30.0 ± 0.2 °C and analyzed at 370 nm.

2.5. MCD spectra

The MCD spectrum of the (imidazole)$_2$-Fe(III)PPIX complex was recorded in 5.64 M aq. DMSO (0.02 M HEPES, pH 7.4). Imidazole stock (0.2 M, pH 7.4) and hemin stock (1 mM in DMSO) solutions were diluted to 0.02 M and 10 μM, respectively, using aq. HEPES (0.02 M, pH 7.4). The spectrum of π–π dimeric Fe(III)PPIX was recorded using a solution made by diluting a stock hemin solution (1 mM in 0.1 M NaOH) with HEPES (0.02 M, pH 7.4), giving a final concentration of π–π dimeric Fe(III)PPIX of 7.5 μM dimer units. To obtain the CQ–Fe(III)PPIX spectrum at pH 7.4, a CQ diphosphate stock solution (1 mM in water) was

added to the same Fe(III)PPIX solution that was used to record the π–π dimer spectrum at pH 7.4. The final concentration of CQ in this solution was 15 μM. The spectrum of μ-[Fe(III)PPIX]$_2$O was reported previously [32].

2.6. Magnetic susceptibility

The magnetic susceptibility of Fe(III)PPIX species in solution was determined using the Evans NMR method as previously described [32]. The solution used to determine the magnetic susceptibility of μ-[Fe(III)PPIX]$_2$O was made by dissolving hematin (3 mg) in 1.20 mL NaOD (0.3 M in D_2O), to which 0.8 mL d_6-DMSO was added. The reference solution was prepared in the same way except no Fe(III)PPIX was added. The value was reported previously in the Supporting Information of reference [32]. The magnetic susceptibility of Fe(III)PPIX in aqueous solution (π–π dimer) was determined for a solution consisting of 1.89 mL hematin solution (3 mg in 0.01 M NaOD) and 0.11 mL phosphoric acid (0.1 M in D_2O), the measured pD of which was 7.2. D_2O was used as the reference solvent. To determine the magnetic susceptibility of the CQ–Fe(III)PPIX complex, a solution consisting of 0.525 mL hematin (3 mg in 0.1 M NaOD) and 1.475 mL CQ (12.2 mg in D_2O), was prepared. The reference solution was made by adding 0.49 mL NaOD (0.1 M) to 1.51 mL of the same CQ solution used to prepare the CQ–Fe(III)PPIX complex. Both solutions had a measured pD of 7.5.

Magnetic susceptibilities of solid Fe(III)PPIX samples were determined using a homemade Evans balance in which the change in mass of a rare earth magnet was related to the magnetic susceptibility of the sample using Eq. (1):

$$\chi_g = \frac{C_{bal}(R_0 - R_1)L}{m \times 10^9} \quad (1)$$

where χ_g is the mass magnetic susceptibility ($cm^3\ g^{-1}$), C_{bal} is the calibration constant of the balance, R_0 is the mass of the magnet (g) when no sample is present, R_1 is the mass of the magnet when the sample is present, L is the length of the sample in the tube (cm) and m is the mass of the sample (g) [33]. The calibration was determined using the magnetic susceptibility constant of a standard, mercury(II) tetrathiocyanatocobaltate(II), as reported by Figgis and Nyholm ($\chi_g = 16.44 \times 10^{-6}\ cm^3\ g^{-1}$) [34]. The diamagnetic contributions of Fe(III)PPIX and CQ were corrected using values of -5.09×10^{-7} and $-4.64 \times 10^{-7}\ cm^3\ g^{-1}$. The former value was determined as described previously [32], while the latter was calculated using Pascal's constants [35]. The molar magnetic susceptibility (χ_m) was calculated by multiplying the corrected χ_g value by the molecular weight of the sample. Each measurement was repeated five times at room temperature.

2.7. Diffusion coefficients

The diffusion coefficients of CQ and the CQ–Fe(III)PPIX complex in aqueous solution (pH 7.4) were determined using the diffusion cell method first reported by Linder et al. [36], following a protocol previously described [28]. For the measurement of CQ diffusion, a CQ working solution (0.6 mM in 0.02 M HEPES, pH 7.4) was prepared by diluting a stock solution (6 mM in 0.2 M HEPES, pH 7.4) ten-fold with water. In the case of CQ–Fe(III)PPIX diffusion, a working solution was prepared by combining 2.5 mL of a hematin stock solution (3 mM in 0.1 M NaOH) and 2.5 mL of the same CQ stock solution used to determine CQ diffusion, and diluting with water to 25 mL. The final concentrations of CQ and Fe(III)PPIX in this working solution were 0.6 mM and 0.3 mM, respectively. Working solutions were loaded into the lower chamber of the diffusion cell and allowed to diffuse for 1 h (CQ) or 2 h (CQ–Fe(III)PPIX) into the upper chamber which contained a HEPES solution (0.02 M, pH 7.4). The diffusion coefficient was calculated using Eq. (2):

$$D = \left(\frac{Ch}{C_0}\right)^2 \frac{\pi}{t} \quad (2)$$

where C is the concentration in the upper chamber, C_0 is the concentration in the lower chamber, h is the height (m) of the upper chamber and t is the time (s) over which the diffusion took place. The concentration in the upper chamber was determined by measuring the absorbance at 342 (CQ) or 385 nm (CQ–Fe(III)PPIX) using extinction coefficients obtained from Beer's Law plots of the working solution (18,560 for CQ and 42,760 $M^{-1}\ cm^{-1}$ per Fe(III)PPIX for the complex). A total of four replicates were recorded for CQ at 297 K, while eight replicates were recorded for the CQ–Fe(III)PPIX complex, four at 297 K and the remaining four at 295 K. Temperature and viscosity corrections were made using the Stokes–Einstein equation in order to normalize diffusion coefficients to 298 K.

3. Results

3.1. Stoichiometry of the CQ–Fe(III)PPIX complex

The interaction of Fe(III)PPIX and CQ was investigated at pH 7.4 and 5.0. At the former pH, Fe(III)PPIX is soluble and thus a Job plot was constructed in order to obtain the binding stoichiometry of the CQ–Fe(III)PPIX complex. In aqueous solution (in the absence of CQ), Fe(III)PPIX has been shown to exist in an equilibrium between the monomeric and π–π dimeric forms. This equilibrium is described by the conditional dimerization constant ($\log K_D = 6.82 \pm 0.06$ at pH 7.4) previously reported by de Villiers et al. [28]. To eliminate possible complications caused by changes in the dimerization state of Fe(III)PPIX, concentrations were chosen at which the π–π dimeric form is dominant. The lowest concentration of Fe(III)PPIX used was 20 μM at which 94% is dimerized (with at least 97% dimerized from the third lowest concentration onwards). As seen from the Job plot in Fig. 1a, at 25 °C a binding stoichiometry corresponding to two equivalents of Fe(III)PPIX per CQ was observed. The same stoichiometry was obtained at 30.0 °C.

This ratio was used in conjunction with spectrophotometric titration data to determine the association constant, K_{obs}, of CQ with Fe(III)PPIX. Meaningful data could only be obtained when Fe(III)PPIX was titrated into a solution of CQ. Data were fitted to the whole spectrum (300–800 nm) using the HypSpec software package [31]. The reverse titration proved mathematically and experimentally intractable. This observation is probably in part related to a previous report by Crespo et al. showing that titration of CQ into a Fe(III)PPIX solution produced different results to that obtained when the reverse titration was performed [14]. The origin of this phenomenon is not understood. In this investigation, such a titration produced results that could not be fitted to the observed stoichiometry obtained from the Job plot.

To account for known processes occurring in solution, both formation of the complex ($CQ{\cdot}M_2$) and dimerization of monomeric Fe(III)PPIX need to be considered according to Eqs. (3) to (6):

$$2M \overset{K_D}{\rightleftharpoons} M_2 \quad (3)$$

$$K_D = \frac{[M_2]}{[M]^2} \quad (4)$$

$$2M + CQ \overset{K_{obs}}{\rightleftharpoons} CQ \cdot M_2 \quad (5)$$

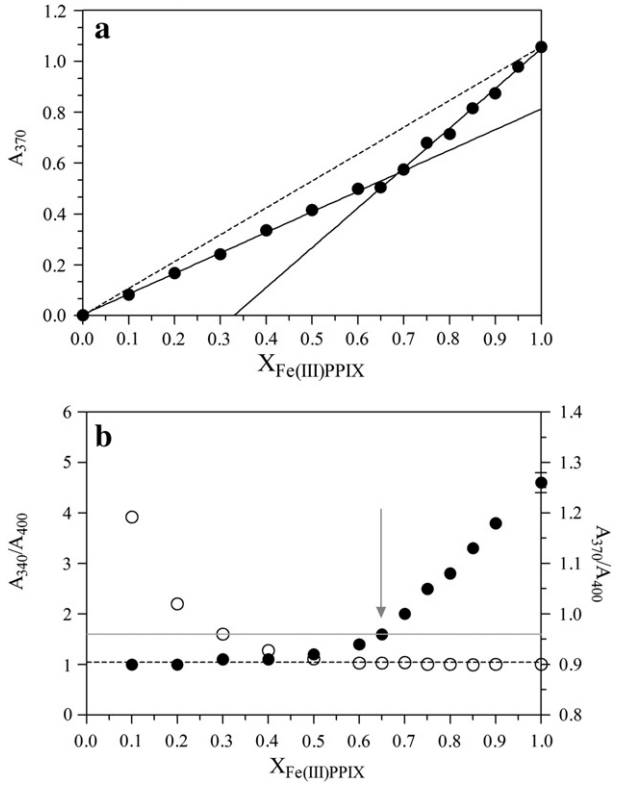

Fig. 1. (a) A typical Job plot obtained for CQ and Fe(III)PPIX in aqueous solution, pH 7.4 and 25 °C (circles). Dashes represent the expected line for dilution of Fe(III)PPIX (Beer's Law). The intersection of the two solid lines is at mole fraction $X_{Fe(III)PPIX} = 0.68 \pm 0.02$ (n = 5), indicating a 1:2 CQ:Fe(III)PPIX binding stoichiometry. (b) Absorbance ratios calculated from spectra used to construct the Job plot shown as a function of $X_{Fe(III)PPIX}$. Open and filled circles represent the ratios A_{340}/A_{400} and A_{370}/A_{400} respectively. The horizontal gray line ($A_{370}/A_{400} = 0.96$) and dashed black line ($A_{340}/A_{400} = 1.05$) represent the absorbance ratios determined from the spectrum of the CQ–Fe(III)PPIX precipitate when dissolved in aqueous solution and refer to the right and left y-axes, respectively. The arrow indicates the stoichiometry that most closely corresponds these absorbance ratios, namely 1:2 CQ:Fe(III)PPIX.

$$K_{obs} = \frac{[CQ \cdot M_2]}{[M]^2[CQ]}. \quad (6)$$

Attempts to fit the data to this model without constraints were unsuccessful owing to the number of parameters. However, since the spectra of CQ, Fe(III)PPIX π–π dimer (M_2) and K_D are independently known, they could be constrained as constants in the fit. This approach resulted in a fitted log K_{obs} of 14.1 ± 0.4 (n = 12). The fit showed that monomeric Fe(III)PPIX (M) never exceeded 2.5% of total Fe(III)PPIX concentration at any point in the titration and averaged 1.4%. Consequently, we made a simplification to the model according to Eqs. (7) to (9):

$$M_2 + CQ \overset{K'}{\rightleftharpoons} CQ \cdot M_2 \quad (7)$$

$$K' = \frac{[CQ \cdot M_2]}{[M_2][CQ]} \quad (8)$$

$$K' \times K_D = \frac{[CQ \cdot M_2]}{[M_2][CQ]} \times \frac{[M_2]}{[M]^2} = \frac{[CQ \cdot M_2]}{[CQ][M]^2} = K_{obs}. \quad (9)$$

Fitting the data to the equilibrium described by Eq. (7) ignores the very small fraction of monomer and permitted free fitting of the smaller number of parameters. These consisted of the spectra of CQ, Fe(III)PPIX dimer and the complex with CQ as well as K'. The value of log K_{obs} obtained in this way was 13.3 ± 0.2 (= logK' + logK_D = {6.5 ± 0.2} + {6.82 ± 0.06}), n = 12. This value was in good agreement with that obtained with the more complex model, but exhibited a smaller error.

Investigation of CQ–Fe(III)PPIX solution interactions at pH 5.0 is hampered by the insolubility of Fe(III)PPIX. Rapid precipitation occurs at this pH and so neither a Job plot nor spectrophotometric titration could be performed. While precipitation of Fe(III)PPIX in the presence of CQ was also observed at this pH, there was a detectible concentration still present in the solution, indicating that the CQ–Fe(III)PPIX complex is more soluble than Fe(III)PPIX alone. This finding supports of the hypothesis of Ursos et al. that antimalarial drugs influence the pH dependent solubility of Fe(III)PPIX [37]. The presence of CQ in the precipitate obtained was confirmed using mass spectrometry where a molecular ion was observed at 320.19 m/z which corresponds to CQH^+ (320.88 $g \cdot mol^{-1}$). No corresponding peak was observed in the spectrum recorded for Fe(III)PPIX precipitated at pH 5.0 in the absence of CQ. This showed that the precipitate obtained at pH 5.0 is a CQ–Fe(III)PPIX complex and not simply Fe(III)PPIX alone. The CQ:Fe(III)PPIX stoichiometry in the solid was probed by dissolving the precipitate in aqueous buffer (pH 7.4) and measuring the ratio of UV–visible absorbances at 340 and 400 nm (A_{340}/A_{400}) and 370 and 400 nm (A_{370}/A_{400}), respectively. These absorbance values were selected because they show a large response at low and high $X_{Fe(III)PPIX}$, respectively. Values determined for the redissolved solid (1.05 and 0.96 for A_{340}/A_{400} and A_{370}/A_{400} respectively) were then compared to corresponding ratios obtained from spectra used to construct the Job plot at pH 7.4. From Fig. 1b, it can be seen that the ratios most closely correspond to those expected for a stoichiometry of 1:2 CQ:Fe(III)PPIX.

3.2. Identification of the Fe(III)PPIX species in the CQ–Fe(III)PPIX complex

The spectrophotometric titration data were best fitted using the simplified model presented in Eqs. (7) to (9). By contrast to previous studies [13,14], the whole spectrum was used to obtain the association constant rather than single wavelengths. The parameters obtained from this fitting procedure include not only the association constant but also the predicted spectra of the unbound reactants and bound product. It should be noted that the three fitted spectra in Fig. 2a–c, amount to average spectra that, when added together at ratios determined by the optimized value of K', are able to reproduce the observed spectroscopic envelope at each point in the titration within experimental error. Furthermore, while the spectra in Fig. 2b and c are directly observed at the beginning and end of the titration, respectively, that shown in Fig. 2a cannot be seen at any point in the titration. As shown in Fig. 2b and a, best-fit spectra of the unbound species corresponded closely to the independently recorded spectra of CQ and the π–π dimer of Fe(III)PPIX, respectively. The fitted spectrum of the product is in agreement with the experimental spectrum of Fe(III)PPIX in the presence of excess CQ (see Fig. 2c). Comparison of the fitted spectrum of the product with that of the π–π Fe(III)PPIX dimer shows poor agreement, while there is much closer agreement with that of μ-$[Fe(III)PPIX]_2O$ albeit with an apparent 20% hypochromism (see Fig. 2d). The fitted spectrum of the CQ complex was identical to that obtained using the more complex model given by Eqs. (3) to (6).

Recently, we reported the use of MCD spectroscopy as a useful tool for the identification of free Fe(III)PPIX species in solution [32]. MCD provides better resolution of underlying bands because it contains both positive and negative Gaussian peaks as well as Gaussian first derivative-shaped peaks. On the other hand, bands making up peaks in UV–visible spectra consist only of positive Gaussian-shaped features. In order to obtain the MCD spectrum of the Fe(III)PPIX species in the CQ–Fe(III)PPIX complex, a spectrum was recorded at pH 7.4. The MCD spectra of a low-spin, monomeric $(imidazole)_2$-Fe(III)PPIX complex, as well as dimeric μ-$[Fe(III)PPIX]_2O$ and π–π Fe(III)PPIX species were also recorded for comparison. All recorded MCD spectra are displayed with their corresponding UV–visible spectra in Fig. 3.

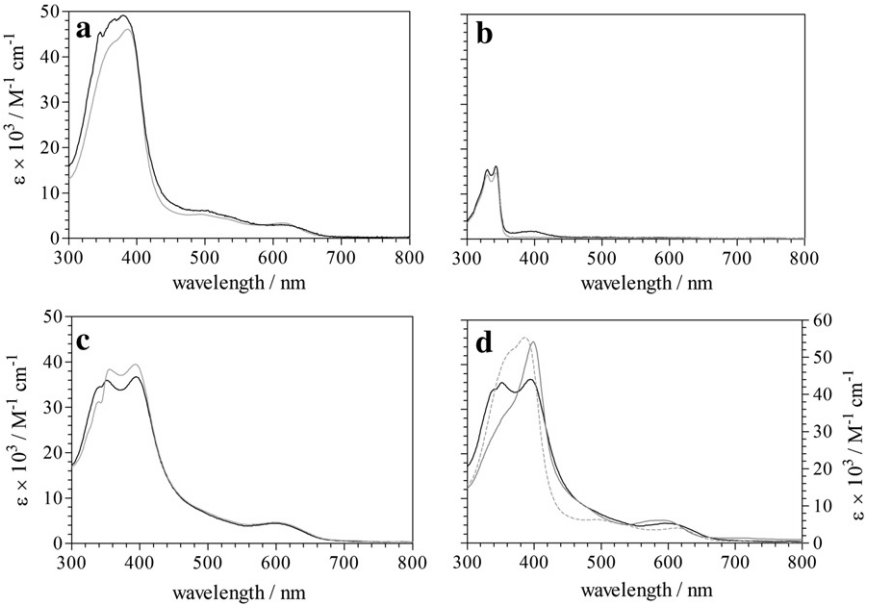

Fig. 2. Experimental and predicted spectra obtained from spectrophotometric titration of CQ with Fe(III)PPIX at pH 7.4 (0.02 M HEPES) and 25 °C according to the simplified equilibrium described by Eq. 7. (a) Predicted spectrum (black) of the free Fe(III)PPIX species compared to the experimental spectrum of π–π dimeric Fe(III)PPIX prepared independently (gray). (b) Predicted spectrum of free CQ (black) compared to that of the initial solution of CQ with no Fe(III)PPIX added (gray). (c) Predicted spectrum of the CQ–Fe(III)PPIX complex (black) compared to that of Fe(III)PPIX in the presence of a CQ concentration twice that of Fe(III)PPIX (gray). (d) Comparison of the predicted spectrum of the CQ–Fe(III)PPIX complex (black) with μ-[Fe(III)PPIX]$_2$O (dark gray) and Fe(III)PPIX π–π dimer (dashed light gray). The extinction coefficients of the complex and π–π dimer refer the left axis while that of μ-[Fe(III)PPIX]$_2$O refers to the right axis. All extinction coefficients are given per mole Fe(III)PPIX.

The UV–visible spectrum of the (imidazole)$_2$-Fe(III)PPIX species is diagnostic of a low-spin complex with two prominent low energy peaks around 533 and 563 nm, and a Soret peak shifted to 411 nm [38,39]. The corresponding MCD spectrum consists of just two prominent derivative-shaped features; one very intense feature centered around 410 nm and the other much less intense centered at 562 nm. For the π–π dimer, as previously noted, the absorbance spectrum exhibits a relatively blunt Soret band at about 386 nm with longer wavelength peaks similar to monomeric H_2O-/HO-Fe(III)PPIX centered around 495, 530 and 614 nm [28]. The corresponding MCD spectrum at long wavelength resembles that previously reported for monomeric H_2O-Fe(III)PPIX with a series of similar features between 450 and 700 nm [32]. Most notably, a fairly broad positive peak close to 480 nm with a less prominent shoulder around 450 nm, and two derivative-shaped features centered around 530 and 620 nm. The latter occur at longer wavelength in monomeric H_2O-Fe(III)PPIX. On the other hand, the Soret region differs markedly from that of monomeric H_2O-Fe(III)PPIX with a much less intense and apparently reversed derivative-shaped feature. The characteristic UV–visible spectrum of μ-[Fe(III)PPIX]$_2$O consists of a sharper Soret peak than the π–π dimer with a prominent high-energy shoulder, very wide low-energy shoulder and a broad peak centered at 590 nm. The MCD spectrum is characterized by three intense Gaussian-shaped peaks of alternating sign centered on 365 nm, an intense derivative-shaped feature around 606 nm and four low intensity peaks between these two main regions. The spectra of the CQ–Fe(III)PPIX complex most closely resemble those of μ-[Fe(III)PPIX]$_2$O. In the UV–visible spectrum, the high-energy side of the Soret band is obscured by peaks arising from the CQ molecule, but the low energy shoulder is remarkably similar to that of μ-[Fe(III)PPIX]$_2$O and bears no resemblance to the low-spin imidazole complex, π–π dimer or previously reported H_2O-Fe(III)PPIX monomer [32]. The single broad peak around 600 nm is similar but not identical to the peak of μ-[Fe(III)PPIX]$_2$O at 590 nm. Thus, as already alluded to above, the UV–visible spectrum suggests that Fe(III)PPIX may occur as μ-[Fe(III)PPIX]$_2$O in the CQ complex. This is further supported by a comparison of MCD spectra which exhibit strikingly similar features including the three Gaussians of alternating sign in the Soret region, the intense derivative-shaped feature in the long wavelength region and the four less intense peaks between the two. Notably, the MCD spectrum does not resemble those of either the low-spin (imidazole)$_2$-Fe(III)PPIX species or the π–π Fe(III)PPIX dimer.

The induction of μ-[Fe(III)PPIX]$_2$O formation by CQ in aqueous solution is further supported by magnetic susceptibility measurements determined using the Evans NMR method (see Table 1 and Fig. 5). The magnetic moment of the CQ–Fe(III)PPIX complex in aqueous solution ($2.25 \pm 0.02\ \mu_B$) was found to differ markedly from the value obtained for the π–π dimeric species in the absence of CQ under the same conditions ($4.8 \pm 0.1\ \mu_B$). Rather, it is in good agreement with that measured for μ-[Fe(III)PPIX]$_2$O ($2.0 \pm 0.1\ \mu_B$) [32].

A similar multi-technique approach was taken to identifying the Fe(III)PPIX species in the CQ–Fe(III)PPIX complex precipitated at pH 5.0. In this case however, IR spectroscopy and magnetic susceptibility measurements using an Evans balance were employed. IR spectra of Fe(III)PPIX obtained at low and high pH and the CQ–Fe(III)PPIX complex precipitated at pH 5.0 are shown in Fig. 4. For comparison, the spectra of CQ (free base), μ-[Fe(III)PPIX]$_2$O and hemin have also been included.

At first glance, the IR spectrum of the CQ–Fe(III)PPIX complex appears to be a simple combination of the spectra obtained for CQ and Fe(III)PPIX precipitated at pH 5.0. Neither the spectrum of the complex nor Fe(III)PPIX resembles that obtained for μ-[Fe(III)PPIX]$_2$O, which has a prominent peak near 1410 cm^{-1} and an intense characteristic υ(Fe–O–Fe) feature at approx. 880 cm^{-1}. Based solely on these results, one may be tempted to conclude that the Fe(III)PPIX species in the precipitated CQ–Fe(III)PPIX complex is not μ-[Fe(III)PPIX]$_2$O but rather is the same species as obtained in the absence of CQ at pH 5.0. However, care needs to be exercised in making such simple qualitative comparisons. The μ-[Fe(III)PPIX]$_2$O species was isolated from strongly alkaline solution as a sodium salt. Under such conditions the propionate groups are fully deprotonated. On the other hand, the CQ–Fe(III)PPIX complex was precipitated at low pH. CQ is doubly protonated at this pH, so in order to produce a neutral CQ–(μ-[Fe(III)PPIX]$_2$O) complex the μ-[Fe(III)PPIX]$_2$O moiety must possess one protonated propionic acid group and one deprotonated propionate group per Fe(III)PPIX molecule.

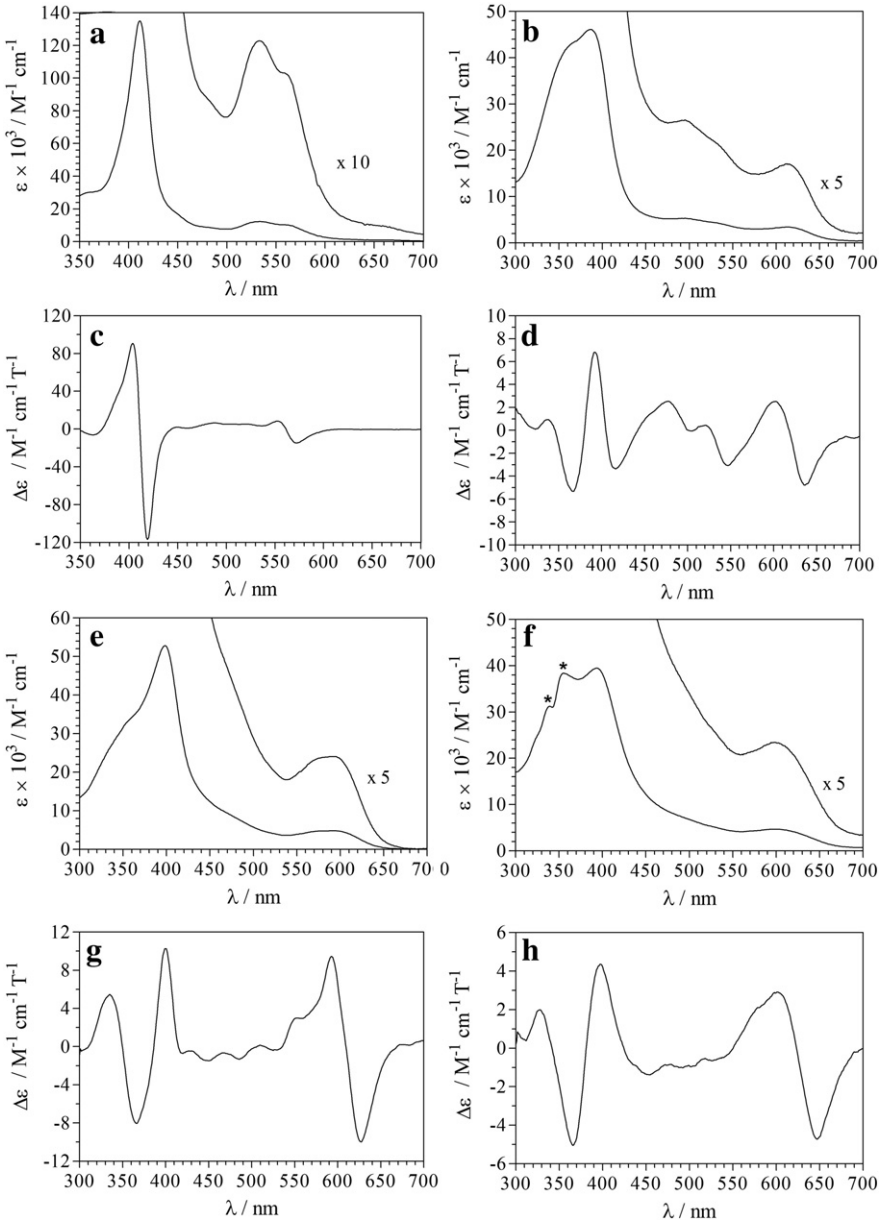

Fig. 3. UV–visible and MCD spectra of Fe(III)PPIX species. (a and c) The (imidazole)$_2$-Fe(III)PPIX complex in 5.64 M aq. DMSO solution, pH 7.4. (b and d) π–π Fe(III)PPIX dimer in aqueous solution, pH 7.4. (e and g) μ-[Fe(III)PPIX]$_2$O in 5.64 M aq. DMSO solution, pH 10. (f and h) CQ–Fe(III)PPIX complex in aqueous solution, pH 7.4. Asterisks in the UV–visible spectrum correspond to CQ peaks. All MCD spectra have been corrected for natural CD.

Table 1
Magnetic moments per Fe(III) center of Fe(III)PPIX species (μ_B) as determined in solution by the Evans NMR method and in the solid state using an Evans balance.

	Fe(III)PPIX species	μ_B
Solution-state	Fe(III)PPIX[a,b]	4.8 ± 0.1
	μ-[Fe(III)PPIX]$_2$O[c]	2.0 ± 0.1
	CQ–Fe(III)PPIX[d,b]	2.25 ± 0.02
Solid-state	Cl–Fe(III)PPIX	6.2 ± 0.2
	Fe(III)PPIX[e,f]	4.0 ± 0.2
	CQ–Fe(III)PPIX[d,f]	2.3 ± 0.1

[a] π–π dimer, axial ligand H_2O/HO^-.
[b] Aqueous, pH 7.4.
[c] 5.64 M aqueous DMSO, pH 10 from reference [32].
[d] 1:2 CQ:Fe(III)PPIX.
[e] π–π dimer, axial ligand H_2O.
[f] Precipitated from aqueous solution at pH 5.

In this respect, it is similar to H_2O-Fe(III)PPIX obtained at pH 5 in the absence of CQ. The propionate υ(COO^-) stretch likely occurs at about 1410 cm^{-1} in μ-[Fe(III)PPIX]$_2$O [32]. The spectrum of HO-Fe(III)PPIX obtained from alkaline aqueous solution by lyophilization also exhibits a υ(COO^-) stretching peak at this position (Fig. 4). By contrast, the IR spectrum of hemin, which possesses only propionic acid groups, displays no such band, but rather a carboxylic acid υ(C═O) stretching peak at approximately 1700 cm^{-1} (Fig. 4). H_2O-Fe(III)PPIX isolated at pH 5 exhibits both signals, as expected. The same is true for the CQ–Fe(III)PPIX complex. As previously reported, [32] H_2O-Fe(III)PPIX displays a characteristic H-O-H bending mode around 1620 cm^{-1}. This peak is absent from μ-[Fe(III)PPIX]$_2$O, but unfortunately cannot be used as a fingerprint in the CQ–Fe(III)PPIX complex because of an overlapping strong CQ peak at about 1613 cm^{-1}. Between 1000 and 650 cm^{-1} the spectroscopic bands of the CQ–Fe(III)PPIX complex are

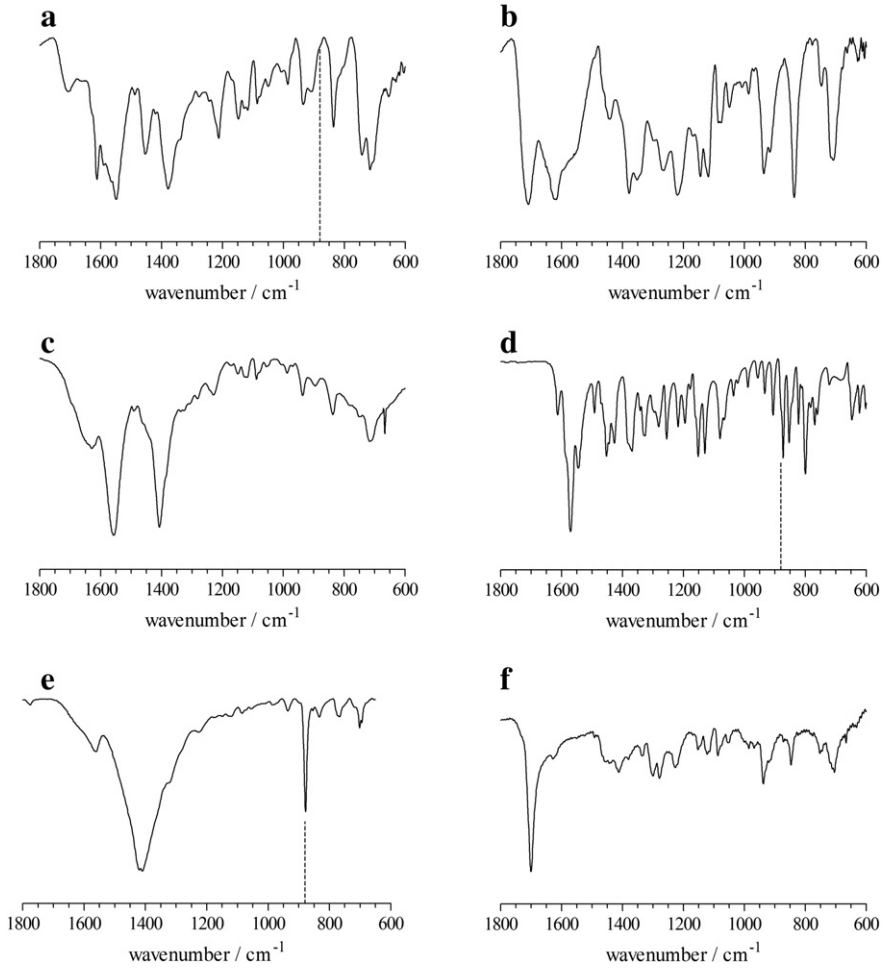

Fig. 4. IR spectra of Fe(III)PPIX species, CQ and CQ–Fe(III)PPIX complex. (a) Fe(III)PPIX precipitated from aqueous solution in the presence of CQ (free base) at pH 5.0. (b) Fe(III)PPIX precipitated from aqueous solution at pH 5.0. (c) Fe(III)PPIX obtained from alkaline aqueous solution. (d) CQ (free base). (e) μ-[Fe(III)PPIX]$_2$O precipitated from an alkaline DMSO solution. (f) Hemin. The vertical dashed line in (a), (d) and (e) marks 880 cm^{-1}, the position of the υ(Fe–O–Fe) peak in μ-[Fe(III)PPIX]$_2$O.

fairly broad. There is no prominent peak around 880 cm^{-1}, but there is a noticeable shoulder at this position. Regrettably, this is inconclusive for identifying the Fe(III)PPIX species present, because CQ exhibits an intense overlapping peak centered at about 873 cm^{-1}. Indeed, with the exception of three peaks that are exclusive to CQ, all of the features in this part of the spectrum are either common to all Fe(III)PPIX species, or overlap with CQ bands. Thus, the use of IR spectroscopy to identify the nature of Fe(III)PPIX in the complex is inconclusive.

Magnetic susceptibility measurements of these solids however, are more definitive (see Table 1). Magnetic moments of the solid samples reproduce the findings observed in aqueous solution at pH 7.4, namely that the Fe(III)PPIX species in the CQ–Fe(III)PPIX complex has a low magnetic moment which is similar to that observed for μ-[Fe(III)PPIX]$_2$O. As a control, the magnetic susceptibility of high-spin (S = 5/2) hemin was also measured. The magnetic moment obtained for this compound (6.2 ± 0.2 μ_B) was close to the expected spin-only value of 5.92 μ_B. Using SQUID magnetometry, Stanek and Dziedzic-Kocurek have determined the *J*-coupling constant for μ-[Fe(III)PPIX]$_2$O to be −110 ± 15 cm^{-1} [40]. The magnetic moment as a function of temperature can be predicted using this *J*-value and is shown in Fig. 5. The value obtained for the CQ–Fe(III)PPIX complex as well as for μ-[Fe(III)PPIX]$_2$O itself agree within reported error with those predicted at the experimental temperature used.

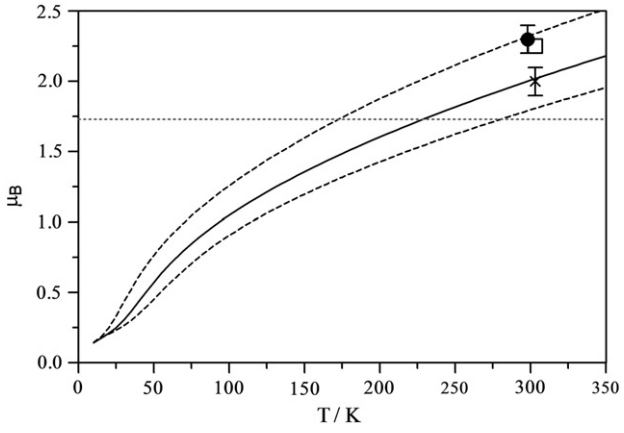

Fig. 5. Predicted temperature dependence of the magnetic moment (μ_B) of μ-[Fe(III)PPIX]$_2$O (solid line) calculated with a *J*-coupling constant of −110 ± 15 cm^{-1} using magnetic susceptibilities obtained from Eq. 14 in reference [40]. Dashed lines represent two standard deviations. The magnetic moments of the solid CQ–Fe(III)PPIX complex at 298 K, the complex in aqueous solution and μ-[Fe(III)PPIX]$_2$O at 303 K determined in our study are represent by the filled circle, open square and cross, respectively. Error bars represent one standard deviation (where there is no error bar, it is smaller than the symbol). The gray dotted line is the expected spin-only value for a low-spin complex with S = 1/2 (1.73 μ_B).

Table 2
Diffusion coefficients (D) normalized to 298 K and calculated molar volumes, V.

	D (10^{-10} m^2 s^{-1})	V (cm^3 mol^{-1})
$(CN)_2$-Fe(III)PPIX[a]	2.2 ± 0.2	485
HO-Fe(III)PPIX[a,b]	1.4 ± 0.1	920
μ-[Fe(III)PPIX]$_2$O[a]	1.6 ± 0.1	907
CQ–Fe(III)PPIX[c]	0.6 ± 0.2	1217 (1:2) 2434 (2:4) 3652 (3:6) 4869 (4:8)
CQ[c]	3.3 ± 0.3	288[d]

[a] Values reported by de Villiers et al. [28].
[b] π–π dimer, pH 10.
[c] Determined in this work.
[d] Predicted using ACD ChemSketch [43].

3.3. Determination of the aggregation state of the CQ–Fe(III)PPIX complex

While the findings described above strongly support the formation of a CQ–μ-[Fe(III)PPIX]$_2$O complex in aqueous solution, they cannot distinguish between monomers, dimers or higher aggregates of this complex. In an attempt to determine the aggregation state, the diffusion coefficient of the complex was measured in aqueous solution using a diffusion cell. The diffusion coefficient of the CQ–Fe(III)PPIX complex is listed in Table 2 along with the value determined for CQ in this work. For comparison, previously reported values for various Fe(III)PPIX species obtained using the same method are also shown [28]. All values have been normalized to 298 K.

As detailed previously [28], an empirical linear relationship between the logarithm of diffusion coefficient, log$D$, and molar volume, log$V$, reported by Gustafson and Dikhut for polyatomic aromatic hydrocarbons [41], has been shown to extend to the monomeric bis-cyano Fe(III)PPIX species, $(CN)_2$-Fe(III)PPIX, as well as the π–π dimeric species in aqueous solution. To increase the number of points in the plot, we have included the diffusion coefficients for several simple substituted aromatic compounds reported by Neisner and Heintz [42]. In addition, the diffusion coefficient of CQ in the absence of Fe(III)PPIX was also determined and incorporated into the plot (Fig. 6). Fitting of this enlarged data set using linear regression produced a statistically significant correlation

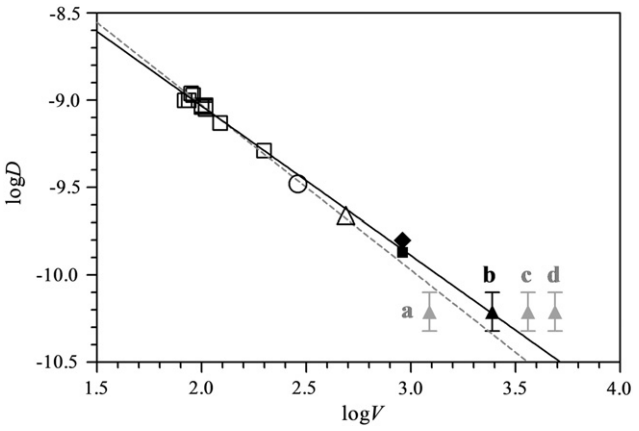

Fig. 6. Dependence of log$D$ (at 298 K) on log$V$. Values for aromatic molecules were obtained from Gustafson and Dikhut [41], and Neisner and Heintz [42] (unfilled squares). Those for $(CN)_2$-Fe(III)PPIX, π–π Fe(III)PPIX dimer and μ-[Fe(III)PPIX]$_2$O (unfilled triangle, filled square and filled diamond respectively) were from de Villiers et al. [28]. Values for CQ (unfilled circle) and CQ–Fe(III)PPIX complex were determined in this study. Various models of the aggregation state of the CQ–Fe(III)PPIX complex are represented by filled triangles. These are (a) 1:2, (b) 2:4, (c) 3:6 and (d) 4:8. The solid line represents the linear regression fitted to the entire aromatic molecule data set together with CQ and $(CN)_2$-Fe(III)PPIX, while the dashed line represents the linear regression previously reported which incorporated only the Gustafson and Dikhut data set together with $(CN)_2$-Fe(III)PPIX. Filled data points were not used in the regression analysis. The models for the CQ–Fe(III)PPIX complex that did not fall on the solid regression line are shown in gray.

($P < 0.0001$, $r^2 = 0.95$) which is shown in Fig. 6 as a solid line alongside the correlation previously reported (dashed line). Incorporating the data for the π–π and μ-oxo dimeric Fe(III)PPIX species into this plot as test molecules, shows that the extrapolated value from the correlation represented by the solid line in Fig. 6 is in close agreement with expectation. Thus this empirical relationship was used to estimate the degree of aggregation of the CQ–Fe(III)PPIX complex.

To position the CQ–Fe(III)PPIX data point on the plot in Fig. 6, the molar volume was required. This was estimated for monomeric (1:2), dimeric (2:4), trimeric (3:6) and tetrameric (4:8) complexes by dividing the molar mass (1567, 3134, 4701 and 6268 g mol^{-1}, respectively) by the predicted density of the complex. The latter was estimated using a weighted average of the density of CQ (predicted using ACD ChemSketch [43]) and Fe(III)PPIX (taken as 1.3753 g cm^{-3} [28]). It can be seen from Fig. 6 that the data point describing the dimeric 2:4 unit is closest to the regression line. This suggests that the CQ–Fe(III)PPIX complex in solution consists of two CQ molecules and two μ-[Fe(III)PPIX]$_2$O dimers, with predicted formula (CQ–μ-[Fe(III)PPIX]$_2$O)$_2$.

4. Discussion

Magnetic susceptibility measurements of the CQ–Fe(III)PPIX complex both in solution and the solid-state unequivocally demonstrated that the complex possesses a low magnetic moment of 2.3 μ_B. This is close to the value determined for μ-[Fe(III)PPIX]$_2$O (2.0 ± 0.1 μ_B) [32]. A Job plot constructed in solution close to pH 7.5, as well as UV–visible spectroscopic measurements obtained by dissolving the solid that had been precipitated at pH 5.0, definitively showed that the mole fraction of Fe(III)PPIX in the complex was 0.68 ± 0.02. This is near to the value of 0.67 expected for a 1:2 CQ:Fe(III)PPIX complex. The complex is strong, with a logK_{obs} of 13.3 ± 0.2 at pH 7.4.

There are only two possible explanations for the low magnetic moment in the CQ–Fe(III)PPIX complex. Either it is low-spin with one unpaired electron, or there are antiferromagnetically coupled iron centers. Low-spin Fe(III)PPIX complexes are observed when two strong-field ligands coordinate to the Fe(III) center, for example in (imidazole)$_2$-Fe(III)PPIX [38,39]. However, this type of complex can be discounted on two grounds. Firstly, the mole fraction of Fe(III)PPIX in such a complex would have to be 0.33, inconsistent with the observed value of 0.68. Secondly, both the UV–visible and MCD spectra of low-spin complexes have characteristic features which are not present in the spectra of CQ–Fe(III)PPIX (see Fig. 3a and c vs. f and h). This leaves strong antiferromagnetic coupling via a bridging ligand linking two high-spin Fe(III) centers as the only explanation for the low magnetic moment. In principle, a number of bridging ligands could be considered. Chloride can be discounted on the basis of its deliberate exclusion from the magnetic susceptibility experiments (which made use of hematin rather than hemin). Phosphate cannot be the bridging group between the paramagnetic centers because it cannot account for the observed strong antiferromagnetic coupling. Direct M–L–M orbital overlap is needed for an efficient superexchange mechanism [44]. Furthermore, it was absent from the solid sample. In our system, this leaves only oxide and hydroxide as feasible bridging ligands. Hydroxo-bridged iron(III) porphyrin complexes are rare, but not unknown [45–47]. J-coupling constants tend to be substantially weaker than those observed for μ-oxo dimers [46,47], in agreement with a theoretical investigation which has shown that protonation of μ-oxo bridging ligands significantly reduces the J-coupling constant between iron(III) centers [48]. Thus, the antiferromagnetic coupling of μ-hydroxo-bridged species would be too weak to account for the low magnetic moment observed in CQ–Fe(III)PPIX. This leaves the μ-oxo dimer of Fe(III)PPIX as the only candidate able to account for the low magnetic moment observed. Such a conclusion is further supported by the close agreement between the observed magnetic moment and the value predicted at experimental temperature using the J-coupling constant of μ-[Fe(III)PPIX]$_2$O (see Fig. 5). This is further substantiated by the close resemblance of the

UV–visible and MCD spectra of CQ–Fe(III)PPIX and μ-[Fe(III)PPIX]$_2$O (see Figs. 2d and 3e and g vs. f and h). In addition, this would also explain the previously reported remarkable similarity between the Mössbauer spectra of CQ–Fe(III)PPIX and μ-[Fe(III)PPIX]$_2$O [22]. A complex of the type CQ–(μ-[Fe(III)PPIX]$_2$O) is thus consistent with both the observed magnetic properties and stoichiometry.

The observation of a 1:2 CQ:Fe(III)PPIX stoichiometry is in agreement with a number of previous studies in aqueous solution. These include Chou et al. who first reported this ratio on the basis of equilibrium dialysis experiments in 50 mM phosphate buffer (pH 7.4) [49]; Constantinidis and Satterlee who performed a UV–visible Job plot at pH 6 using urohemin [50]; NMR relaxation studies at pH 6.5 by Leed et al. and Schwedhelm et al. [19,23]; and most recently a UV–visible Job plot by Crespo et al. in 10 mM phosphate buffer (pH 7.4) [14]. It is notable that studies reporting higher ratios (1:4–1:8) were all performed using ITC, usually with 0.25 M phosphate buffer and often with relatively high concentrations of salts (e.g. 0.15 M KCl) [24,25,51]. Elevated ionic strengths have previously been reported to be able to induce higher aggregation of μ-[Fe(III)PPIX]$_2$O [29]. Regardless of the reason for this discrepancy, it is clear from the Job plot (Fig. 1a) and even more strikingly from the absorbance ratios of the redissolved CQ–Fe(III)PPIX precipitate (Fig. 1b), that stoichiometries of 1:4 and higher fall well outside our experimental error and can therefore be excluded. A number of authors have suggested that the CQ–Fe(III)PPIX complex in aqueous solution involves μ-[Fe(III)PPIX]$_2$O [19,20,23,24,26,52]. While some substantiated this claim with magnetic moment measurements [20,21,23], in most cases it was based on the supposition that μ-[Fe(III)PPIX]$_2$O is the predominant species in aqueous solution. Several recent studies have shown that this is not the case, but rather that it is predominantly a π–π dimer [14,28,29]. This is further supported by the MCD spectrum shown in Fig. 3d which dramatically differs from that of μ-[Fe(III)PPIX]$_2$O (Fig. 3g). Regardless of this recent evidence, there is still a widespread misconception that μ-[Fe(III)PPIX]$_2$O is the major species in aqueous solution [27]. This is an important point because the current findings show that CQ induces formation of μ-[Fe(III)PPIX]$_2$O, rather than simply binding to preformed μ-[Fe(III)PPIX]$_2$O. Thus in the equilibrium described by Eq. 7 above, M_2 on the left-hand side represents Fe(III)PPIX π–π dimer, while on the right-hand side it represents μ-[Fe(III)PPIX]$_2$O. Indeed, in the fitting of complete spectra to the spectrophotometric titration data, it was quite evident that the free Fe(III)PPIX species is the π–π dimer (Fig. 2a). A second misconception that needs to be dispelled is the idea that the low magnetic moment of μ-[Fe(III)PPIX]$_2$O arises from the Fe(III) centers existing in a low-spin state with one unpaired electron ($S = 1/2$). This is not the case. Rather, the low magnetic moment arises from quantum mechanical coupling between the five unpaired electrons on each iron center in a temperature-dependent manner (see prediction in Fig. 5). Such a system would be diamagnetic at 0 K, but becomes thermally decoupled with increasing temperature [40]. In the case of μ-[Fe(III)PPIX]$_2$O, its J-coupling constant gives rise to a magnetic moment at 298 K coincidentally similar, but not identical to that of a low-spin complex ($\mu_B = 2.06$ versus 1.73, see Fig. 5 solid black line vs. gray dotted line).

Recent uncertainty about whether μ-[Fe(III)PPIX]$_2$O is present in the CQ–Fe(III)PPIX complex can be ascribed to the reported absence of the Fe–O–Fe antisymmetric stretching band in the IR spectrum around 880 cm^{-1} [15]. Indeed, in the present study, we confirm the absence of a prominent band at this position (Fig. 4a). However, given the incontrovertible magnetic evidence obtained from the very same sample for the presence of μ-[Fe(III)PPIX]$_2$O, we can only conclude that this peak is not a definitive marker. There is precedence for the apparent disappearance of this peak. Ercolani et al. demonstrated the existence of two interconvertible forms of an iron(III)phthalocyanin μ-oxo dimer, one of which lacked the characteristic υ(Fe–O–Fe) frequency despite definitive magnetic and compositional evidence that it was indeed a μ-oxo dimer [53]. Lever and coworkers also reported the absence of similar IR absorptions in some μ-oxo manganese(III)phthalocyanins [54]. These authors put forward no hypotheses to explain the absence of the band. While a similar phenomenon may occur here, we suspect that it is more likely that the peak is present, but that it is a shoulder. Furthermore, owing to overlap with a CQ band at a similar position it is poorly resolved.

Although both the Job plot and UV–visible spectroscopic measurements on redissolved precipitate show that the CQ:Fe(III)PPIX ratio in the complex is 1:2, they do not provide information on its aggregation state. In other words, these techniques are not able to distinguish between 1:2, 2:4 and 3:6 complexes or even higher aggregates. There have been differing opinions regarding this matter. For example, Moreau et al. proposed that the CQ–Fe(III)PPIX complex stacks in very large aggregates consisting of alternating CQ and μ-[Fe(III)PPIX]$_2$O molecules [52], while Schwedhelm et al., proposed a 2:4 complex [23]. This problem is difficult to investigate because it is not easily addressed by spectroscopic techniques. Therefore, we have attempted to probe the aggregation state using diffusion measurements. The Stokes–Einstein relationship is sometimes used to relate diffusion coefficients to molecular size. However, this equation was developed to describe the diffusion of macroscopic colloids and does not strictly apply to the molecular scale, especially in strongly solvating systems such as water. Empirical relationships such as the Othmer–Thakar, Hayduk–Laudie, Wilke–Chang and Scheibel equations have been proposed to predict molecular diffusion coefficients [55–58]. More recent correlations observed by Gustafson and Dikhut led to improved predictions for planar extended aromatic systems [41]. We have previously shown this to be of value for Fe(III)PPIX species [28]. Using this approach, with the addition of further empirical data for both aromatic systems and Fe(III)PPIX species, we found that the 2:4 complex best fitted the correlation line (see Fig. 6). We therefore tentatively identify the complex as (CQ–μ-[Fe(III)PPIX]$_2$O)$_2$. It must, however, be recognized that the empirical nature of this approach together with fairly large experimental errors makes it impossible to completely exclude either the 1:2 or 3:6 aggregates. Large aggregates can however be discounted.

As a final point, we note that our proposed complex, (CQ–μ-[Fe(III)PPIX]$_2$O)$_2$, is similar to that suggested by Schwedhelm et al. [23]. However, the structure proposed by these authors involving two adjacent μ-[Fe(III)PPIX]$_2$O linked by reciprocal propionate-Fe(III) coordination bonds and capped with CQ, is inconsistent with IR evidence. As in hemozoin/β-hematin, coordination of propionate groups to Fe(III) should give rise to intense bands at around 1660 and 1210 cm^{-1}. Indeed, they are striking markers of such an interaction in hemozoin [59], but are clearly completely absent from the spectrum of the CQ–Fe(III)PPIX complex (Fig. 4b). In fact, Schwedhelm et al. proposed such a structure to account for the low magnetic moment of the complex, which they erroneously ascribed to a low-spin state which they claimed required entirely six-coordinate Fe(III) centers. As we have noted above, the low magnetic moment in fact arises from antiferromagnetic coupling of high-spin Fe(III) centers. Moreover, six-coordinate Fe(III)PPIX is only low-spin with strong-field ligands and would not be likely with weak-field oxide and propionate π-donor groups.

5. Conclusions

Magnetic susceptibility measurements together with UV–visible and MCD observations convincingly demonstrate that CQ induces formation of the μ-oxo dimer of Fe(III)PPIX, forming a CQ–Fe(III)PPIX complex with a 1:2 stoichiometry. This occurs both in solution at pH 7.5 and in the solid precipitated at pH 5.0 (at least under the preparation conditions used in this study). The IR band near 880 cm^{-1} that has been proposed to be characteristic of the μ-oxo dimer species is not a definitive marker in this system. It is not resolved in the sample of CQ–Fe(III)PPIX which magnetic and spectroscopic measurements showed could only be antiferromagnetically coupled. Determination of the aggregation state of the complex is less conclusive, but diffusion data suggest

that the best model is (CQ–μ-[Fe(III)PPIX]$_2$O)$_2$. At this stage, we are not offering a structural hypothesis for the complex. Rather, based on the current findings, this is being investigated in a detailed molecular dynamics study supported by EXAFS. The results will be reported in the near future.

Finally, we would like to stress that we do not propose that the complex described here is necessarily directly responsible for hemozoin inhibition. Indeed, recent studies from our group have lent support to the proposal that CQ acts by inhibiting the fast-growing face of the hemozoin crystal [7,60]. Nonetheless, it is likely that the complex will form as a consequence of inhibition of hemozoin formation. It may well then play an important role in the subsequent distribution of Fe(III)PPIX in the malaria cell and hence influence its toxicity to the parasite.

Abbreviations

CQ	chloroquine
EXAFS	extended X-ray absorption fine structure
Fe(III)PPIX	ferriprotoporphyrin IX
MCD	magnetic circular dichroism
ITC	isothermal titration calorimetry

Acknowledgments

This material is based upon the work supported in part by the National Research Foundation of South Africa (NRF). Any opinion, findings and conclusions or recommendations expressed in this material are those of the authors and do not necessarily reflect the views of the National Research Foundation. We also acknowledge the support of the Medical Research Council of South Africa and the University of Cape Town (UCT). DK acknowledges the NRF, UCT and Kevin J. Naidoo (through the South African Research Chairs Initiative of the Department of Science and Technology and NRF) for financial support.

References

[1] R.L. Summers, M.N. Nash, R.E. Martin, Cell. Mol. Life Sci. 69 (2012) 1967–1995.
[2] A. Ecker, A.M. Lehane, C. Clain, D.A. Fidock, Trends Parasitol. 28 (2012) 504–514.
[3] R.E. Martin, R.V. Marchetti, A.I. Cowan, S.M. Howitt, S. Bröer, K. Kirk, Science 325 (2009) 1680–1682.
[4] D. van Schalkwyk, T.J. Egan, Drug Resist. Updat. 9 (2006) 211–226.
[5] D.C. Warhurst, J.C. Craig, I.S. Adagu, R.K. Guy, P.B. Madrid, Q.L. Fivelman, Biochem. Pharmacol. 73 (2007) 1910–1926.
[6] F. Dubar, T.J. Egan, B. Pradines, D. Kuter, K.K. Ncokazi, D. Forge, J.-F. Paul, C. Pierrot, H. Kalamou, J. Khalife, E. Buisine, C. Rogier, H. Vezin, I. Forfar, C. Slomianny, X. Trivelli, S. Kapishnikov, L. Leiserowitz, D. Dive, C. Biot, ACS Chem. Biol. 6 (2011) 275–287.
[7] J.M. Combrinck, T.E. Mabotha, K.K. Ncokazi, M.A. Ambele, D. Taylor, P.J. Smith, H.C. Hoppe, T.J. Egan, ACS Chem. Biol. 8 (2013) 133–137.
[8] R. Hayward, K.J. Saliba, K. Kirk, J. Cell Sci. 119 (2006) 1016–1025.
[9] T.J. Egan, J.M. Combrinck, J. Egan, G.R. Hearne, H.M. Marques, S. Ntenteni, B.T. Sewell, P.J. Smith, D. Taylor, D.A. van Schalkwyk, J.C. Walden, Biochem. J. 365 (2002) 343–347.
[10] R. Buller, M.L. Peterson, Ö. Almarsson, L. Leiserowitz, Cryst. Growth Des. 2 (2002) 553–562.
[11] C.H. Kaschula, T.J. Egan, R. Hunter, N. Basilico, S. Parapini, D. Taramelli, E. Pasini, D. Monti, J. Med. Chem. 45 (2002) 3531–3539.
[12] F. Dubar, S. Bohic, C. Slomianny, J.-C. Morin, P. Thomas, H. Kalamou, Y. Guérardel, P. Cloetens, J. Khalife, C. Biot, Chem. Commun. 48 (2012) 910–912.
[13] T.J. Egan, W.W. Mavuso, D.C. Ross, H.M. Marques, J. Inorg. Biochem. 68 (1997) 137–145.
[14] M.P. Crespo, L. Tilley, N. Klonis, J. Biol. Inorg. Chem. 15 (2010) 1009–1022.
[15] M. Asghari-Khiavi, J. Vongsvivut, I. Perepichka, A. Mechler, B.R. Wood, D. McNaughton, D.S. Bohle, J. Inorg. Biochem. 105 (2011) 1662–1669.
[16] T. Frosch, B. Küstner, S. Schlücker, A. Szeghalmi, M. Schmitt, W. Kiefer, J. Popp, J. Raman Spectrosc. 35 (2004) 819–821.
[17] G.T. Webster, D. McNaughton, B.R. Wood, J. Phys. Chem. B 113 (2009) 6910–6916.
[18] M.S. Walczak, K. Lawniczak-Jablonska, A. Wolska, A. Sienkiewicz, L. Suárez, A.J. Kosar, D.S. Bohle, J. Phys. Chem. B 115 (2011) 1145–1150.
[19] A. Leed, K. DuBay, L.M.B. Ursos, D. Sears, A.C. de Dios, P.D. Roepe, Biochemistry 41 (2002) 10245–10255.
[20] L.B. Casabianca, D. An, J.K. Natarajan, J.N. Alumasa, P.D. Roepe, C. Wolf, A.C. de Dios, Inorg. Chem. 47 (2008) 6077–6081.
[21] L.B. Casabianca, J.B. Kallgren, J.K. Natarajan, J.N. Alumasa, P.D. Roepe, C. Wolf, A.C. de Dios, J. Inorg. Biochem. 103 (2009) 745–748.
[22] P.A. Adams, P.A.M. Berman, T.J. Egan, P.J. Marsh, J. Silver, J. Inorg. Biochem. 63 (1996) 69–77.
[23] K.F. Schwedhelm, M. Horstmann, J.H. Faber, Y. Reichert, M. Büchner, G. Bringmann, C. Faber, Open Spec. J. 2 (2008) 10–18.
[24] A. Dorn, S.R. Vippagunta, H. Matile, C. Jaquet, J.L. Vennerstrom, R.G. Ridley, Biochem. Pharmacol. 55 (1998) 727–736.
[25] K. Bachhawat, C.J. Thomas, N. Surolia, A. Surolia, Biochem. Biophys. Res. Commun. 276 (2000) 1075–1079.
[26] S.R. Vippagunta, A. Dorn, R.G. Ridley, J.L. Vennerstrom, Biochim. Biophys. Acta 1475 (2000) 133–140.
[27] A.P. Gorka, A.C. De Dios, P.D. Roepe, J. Med. Chem. 56 (2013) 5231–5246.
[28] K.A. de Villiers, C.H. Kaschula, T.J. Egan, H.M. Marques, J. Biol. Inorg. Chem. 12 (2007) 101–117.
[29] C. Asher, K.A. de Villiers, T.J. Egan, Inorg. Chem. 48 (2009) 7994–8003.
[30] S.B. Brown, P. Jones, I.R. Lantzke, Nature 223 (1969) 960–961.
[31] P. Gans, A. Sabatini, A. Vacca, Talanta 43 (1996) 1739–1753.
[32] D. Kuter, G.A. Venter, K.J. Naidoo, T.J. Egan, Inorg. Chem. 51 (2012) 10233–10250.
[33] D.F. Evans, J. Phys. E Sci. Instrum. 7 (1974) 247–249.
[34] B.N. Figgis, R.S. Nyholm, J. Chem. Soc. (1958) 4190–4191.
[35] G.A. Bain, J.F. Berry, J. Chem. Educ. 85 (2008) 532–536.
[36] P.W. Linder, L.R. Nassimbeni, A. Polson, A.L. Rodgers, J. Chem. Educ. 53 (1976) 330–332.
[37] L.M.B. Ursos, K.F. DuBay, P.D. Roepe, Mol. Biochem. Parasitol. 112 (2001) 11–17.
[38] H.M. Marques, O.Q. Munro, M.L. Crawcour, Inorg. Chim. Acta 196 (1992) 221–229.
[39] D. Kuter, K. Chibale, T.J. Egan, J. Inorg. Biochem. 105 (2011) 684–692.
[40] J. Stanek, K. Dziedzic-Kocurek, J. Magn. Magn. Mater. 322 (2010) 999–1003.
[41] K.E. Gustafson, R.M. Dickhut, J. Chem. Eng. Data 39 (1994) 281–285.
[42] R. Niesner, A. Heintz, J. Chem. Eng. Data 45 (2000) 1121–1124.
[43] Advanced Chemistry Development Inc., Toronto, ON, Canada, 2013.
[44] J.B. Goodenough, Magnetism and the Chemical Bond, Wiley, New York, 1963, pp. 170–172.
[45] W.R. Scheidt, B. Cheng, M.K. Safo, F. Cukiernik, J.-C. Marchon, P.G. Debrunner, J. Am. Chem. Soc. 114 (1992) 4420–4421.
[46] D.R. Evans, R.S. Mathur, K. Heerwegh, C.A. Reed, Z. Xie, Angew. Chem. Int. Ed. 36 (1997) 1335–1337.
[47] S.K. Ghosh, S.P. Rath, J. Am. Chem. Soc. 132 (2010) 17983–17985.
[48] Z. Chen, Z. Xu, L. Zhang, F. Yan, Z. Lin, J. Phys. Chem. A 105 (2001) 9710–9716.
[49] A.C. Chou, R. Chevli, C.D. Fitch, Biochemistry 19 (1980) 1543–1549.
[50] I. Constantinidis, J.D. Satterlee, J. Am. Chem. Soc. 110 (1988) 4391–4395.
[51] S.R. Cheruku, S. Maiti, A. Dorn, B. Scorneaux, A.K. Bhattacharjee, W.Y. Ellis, J.L. Vennerstrom, J. Med. Chem. 46 (2003) 3166–3169.
[52] S. Moreau, B. Perly, C. Chachaty, C. Deleuze, Biochim. Biophys. Acta 840 (1985) 107–116.
[53] C. Ercolani, M. Gardini, F. Monacelli, G. Pennesi, G. Rossi, Inorg. Chem. 22 (1983) 2584–2589.
[54] G.W. Rayner Canham, A.B..P. Lever, Inorg. Nucl. Chem. Lett. 9 (1973) 513–517.
[55] D.F. Othmer, M.S. Thakar, Ind. Eng. Chem. 45 (1953) 589–593.
[56] W. Hayduk, H. Laudie, AIChE J 20 (1974) 611–615.
[57] C.R. Wilke, P. Chang, AIChE J 1 (1955) 264–270.
[58] E.G. Scheibel, Ind. Eng. Chem. 46 (1954) 2007–2008.
[59] A.F.G. Slater, W.J. Swiggard, B.R. Orton, W.D. Flitter, D.E. Goldberg, A. Cerami, G.B. Henderson, Proc. Natl. Acad. Sci. U. S. A. 88 (1991) 325–329.
[60] J. Gildenhuys, T. le Roex, T.J. Egan, K.A. de Villiers, J. Am. Chem. Soc. 135 (2013) 1037–1047.